Journal of Sustainability Science and Management
Volume 20 Number 9, September 2025: 1807-1818

eISSN: 2672-7226

DEVICE PERFORMANCE FOR CTS-BASED THIN FILM SOLAR CELL USING SCAPS-1D SIMULATOR

FAKHRUL MD ISLAM[1,2], MOHAMMAD AMINUL ISLAM[3], DILIP KUMAR SARKAR[4] AND NADHRAH MD YATIM[1]*

[1]Energy Materials Consortium, Faculty of Science and Technology, Universiti Sains Islam Malaysia, 71800 Nilai, Negeri Sembilan, Malaysia. [2]Daffodil International University, Birulia 1216, Dhaka, Bangladesh. [3]Department of Electrical Engineering, University of Malaya, 50603 Kuala Lumpur, Wilayah Persekutuan Kuala Lumpur, Malaysia. [4]Applied Chemistry and Chemical Engineering, University of Rajshahi, Rajshai 6205, Bangladesh.

**Corresponding author: nadhrah@usim.edu.my*
http://doi.org/10.46754/jssm.2025.09.004
Submitted: 30 August 2024 Revised: 30 November 2024 Accepted: 8 December 2024 Published: 15 September 2025

Abstract: Thin-film (TF) solar cells have recently gained attention due to their high energy conversion efficiency and sustainability to meet rising energy demands. The absorber layer is an important part of solar cells and is responsible for light absorption. Popular absorber layers used in TF solar cells include $Cu(In,Ga)Se_2$ (CIGS), cadmium telluride (CdTe), and Copper Zinc Tin Sulphide (CZTS). However, these materials have drawbacks due to the toxicity of the materials used, scarcity, and/or high fabrication costs. To address these issues, this study proposes Copper Tin Sulphide (CTS) as a safer and more abundant alternative for TF solar cell applications. Numerical models for the absorber layer (CTS) and window layer (CdS) were conducted using a Solar Cell Capacitance Simulator (SCAPS-1D) to determine the optimised design. The thickness and Carrier Concentration (CC) of both CTS and CdS layers were varied to achieve an optimised energy band gap (E_g). Data from these optimisations were used to predict the photovoltaic (PV) device output. The device demonstrated a conversion efficiency (η) as high as 22.56%, with short-circuit current (J_{sc}) of 35.23 mA/cm^2, open-circuit current (V_{oc}) of 0.827V and Fill Factor (FF) of 77.32%, achieved with a CTS layer of 1´10^{18} cm^{-3} carrier concentration, 1,500 nm thickness, and 1.2 eV energy band gap, combined with a CdS layer of 1´10^{18} cm^{-3} carrier concentration and 120 nm thickness. The highest reported experimental efficiencies for CTS-based solar cells are 5.1% (Na-doped CTS) and 6.0% (Ge-alloyed CTS). These findings indicate significant potential for improving current TF PV devices. Further experimental investigation is recommended, and successful outcomes may contribute to the long-term sustainability of solar cell technology.

Keywords: CTS, solar cell, numerical simulation, SCAPS-1D, absorber layer.

Introduction

Solar energy is a preferred alternative to fossil fuels due to its environmental sustainability. However, widespread adoption of solar cells is limited by factors such as high cost, bulkiness, and toxicity. Current research focuses on developing more sustainable and cost-effective solar technologies. Compared to conventional silicon wafers, thin-film (TF) solar cells offer advantages including reduced material usage, lower environmental impact, and compatibility with flexible substrates such as metal or plastic foils, making them suitable for diverse applications, from building materials to portable devices. A key challenge in this field remains the selection of suitable materials, as their properties directly influence power conversion efficiency.

Chalcogenide compounds from group I-IV-VI such as Cu-Sn-S, show promise for solar applications due to their abundance and non-toxic composition (Adelifard *et al*., 2012). To date, CTS-based TF solar cells have reached efficiencies of up to 5.1% with Na doping (Chantana *et al*., 2020) and 6.7% with Ge alloying (Umehera *et al*., 2016). Various semiconducting phases exist in CTS, including Cu_4SnS_4, Cu_2SnS_3, Cu_3SnS_4, $Cu_2Sn_3S_7$, and $Cu_4Sn_7S_{16}$ (Chen *et al*., 2003; Friechter *et al*., 2003), with Cu_2SnS_3 and Cu_3SnS_4 identified as the most promising due to their high absorption coefficients and ideal direct band gaps (Bouaziz *et al*., 2009).

Cu_2SnS_3 thin films have been fabricated through a variety of chemical and physical processes, including chemical baths (Taher *et al*., 2015), vacuum evaporation (Robles *et al*., 2015), electrodeposition (Mathews *et al*., 2013), spray pyrolysis (Adelifard *et al*., 2012), SILAR (Guan *et al*., 2013), magnetron sputtering (Akcay *et al*., 2023), and electron beam evaporation (Aihara *et al*., 2013). These films exhibit a range of crystal structures, including cubical (Amlouk *et al*., 2013), tetragonal (Chen & Ma, 2013), hexagonal (Wu *et al*., 2007), monoclinic (Berg *et al*., 2012), and triclinic (Han *et al*., 2014). To reduce resource depletion and environmental effects, it is important to improve light absorption, carrier transport qualities, long-term stability, degradation resistance, fabrication energy efficiency, and recyclability. Thin film solar cells have the potential to play a significant role in the development of clean and sustainable energy sources by addressing these issues and emphasising sustainability across their whole life cycle.

This study aims to simulate an affordable and environmentally sustainable absorber layer for TF solar cells. The effects of thickness, band gap, and carrier concentration in both the absorber and the buffer layer on photovoltaic performance are analysed suing the Solar Cell Capacitance Simulator (SCAPS-1D). The tool is widely used for solar cell modelling due to its ease of use, comprehensive physics models, flexibility, accurate performance predictions, ability to analyse loss mechanisms, and cost-effectiveness. Despite its strength, SCAPS-1D operates in one dimension and assumes ideal material properties, limiting its ability to reflect three-dimensional effects and real-word imperfections.

While this study introduces a new optimisation method for CTS and CdS layers, it is acknowledged that real-world efficiency is also influenced by fabrication methods, material quality, contact resistance, optical losses, temperature effects, and other external factors. Nevertheless, SCAPS-1D serves as a valuable tool for estimating the theoretical maximum efficiency and guiding experimental efforts.

Materials and Methods

The performance of solar cells can be predicted using numerical modelling, which also helps accelerate the manufacturing process. In this study, simulations were conducted using SCAPS-1D to examine the effects of changing sample properties, where several measurements have been (more or less) quantitatively defined. The presence or absence of specific properties or the fluctuations of all attributes within a range of values was used to identify ideal value for maximising solar cell efficiency.

The device structure of the solar cell construction used in this study is shown in Figure 1. The model consists of a Mo/CTS/CdS/iZnO/AZO configuration, in which p-type CTS serves as the absorber layer and n-type CdS as the buffer. Table 1 presents the parameters used in the SCAPS 1D simulation, based on values from standard solar cell devices reported by Fernandes *et al*. (2010), Jin *et al*. (2017), Hossain *et al*. (2018), and Jiang *et al*. (2019). For optimisation, the properties of other layers were kept constant while the CTS absorber's layer thickness (t), Carrier Concentration (CC), and Energy band gap (E_g) were varied as shown in Table 2 (a). Once the optimum value for the CTS absorber layer was determined, optimisation for the CdS buffer layer was performed by varying its Carrier Concentration (CC) and thickness (t) according to Table 2 (b) while keeping CTS parameters constant. These optimum values were then used to estimate the overall device performance of the solar cells.

Due to software limitations, the effects of series and shunt resistance were not considered. The band discontinuity at the material interfaces was assumed to be minimal and was thus ignored. The AM 1.5 solar spectrum was used in this simulation and the initial temperature was set to 300 K. To assess device performance,

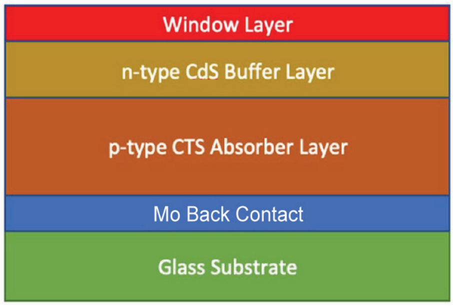

Figure 1: The basic structure of a constructed solar cells device

Table 1: Parameters used in SCAPS-1D numeral modelling
(Fernandes *et al*., 2010; Jin *et al*., 2017; Hossain *et al*., 2018; Jiang *et al*., 2019)

	Unit	CTS	CdS	ZnO	i-ZnO
Thickness (uniform layer)	nm	1500*	40*	50	200
Band gap, E_g	eV	1.20*	2.42	3.35	3.35
Electron affinity, χ	eV	4.71	4.5	4.4	4.4
Dielectric Permittivity, ε_r	relative	10	10	9	9
CB density of state, N_C	cm^{-3}	2·2´10^{18}	1·8´10^{18}	2·2´10^{18}	2·2´10^{18}
VB density of state, N_V	cm^{-3}	1·80´10^{19}	2·40´10^{19}	1·80´10^{19}	1·80´10^{19}
Electron thermal velocity	cm/sec	1·00´10^{7}	1·00´10^{7}	1·00´10^{7}	1·00´10^{7}
Hole thermal velocity	cm/sec	1·00´10^{7}	1·00´10^{7}	1·00´10^{7}	1·00´10^{7}
Electron mobility, μ_e	cm^2/vs	1·00´10^{2}	1·00´10^{2}	1·00´10^{2}	1·00´10^{2}
Hole mobility, μ_h	cm^2/vs	8·00´10^{1}	2·50´10^{1}	2·50´10^{1}	2·50´10^{1}
Uniform donor density (heavily doped), N_D	cm^{-3}	0	1.00´10^{15*}	1·00´10^{12}	1·00´10^{17}
Uniform acceptor density (lightly doped), N_A	cm^{-3}	1.00´10^{18*}	0	1.00´10^{13}	0
Absorption coefficient, a	cm^{-1}	2.00´10^{4}	0	0	0
Defect-1:					
(a) Defect density (uniform), N_t	cm^{-3}	single donor	single acceptor	single acceptor	single neutral
(b) Capture cross-section (holes & electrons), α	cm^{-2}	10^{-15}	10^{-15}	10^{-15}	10^{-15}

* varied as shown in Table 2.
* Conduction Band (CB); Valence Band (VB).

the complete solar cell device structure was simulated. The model starts with a molybdenum (Mo) back contact on a glass substrate, followed by p-CTS and n-CdS layers. These are topped by i-ZnO and ITO, which serve as window layers for protection and phonon absorption.

In this simulation, only the CTS and CdS layers were optimised while other properties

Table 2: Parameter used in (a) CTS layer and (b) CdS layer

	Unit	(a) CTS	(b) CdS
Thickness (uniform layer)	nm	300 - 1,500	40 - 120
Band gap, E_g	eV	0.90 - 1.20	2.42
Uniform donor density (heavily doped), N_D	cm^{-3}	0	10^{12} - 10^{18}
Uniform acceptor density (lightly doped), N_A	cm^{-3}	10^{13} - 10^{18}	0

were kept constant. Optimum values for the CTS and CdS layers were determined based on key photovoltaic performance parameters, which are open-circuit voltage (V_{oc}), short-circuit current density (J_{sc}), Fill Factor (FF), and efficiency (η), within the SCAPS-1D operating temperature. Figure 2 shows the schematic diagram of the simulated solar cell.

Results and Discussion

CTS Absorber Layer – Effect of Thickness

The CTS absorber layer is the core of the solar cell, as it absorbs most photons, which in turn drives electrons into the conduction band to generate photocurrent. When the layer is too thin, its absorption capacity is reduced, leading to lower power conversion efficiency. Conversely, overly thick absorber layers hinder charge carriers from reaching the electrodes, resulting in recombination losses and decreased performance. Increasing the carrier concentration in the absorber layer enhances photocurrent generation.

To determine the optimum thickness of the CTS layer, its thickness was varied from 300 nm to 1,500 nm. During this variation in SCAPS-1D, the characteristics of other layers are maintained constant and the band gap of the absorber was fixed at 1.20 eV. The effects of varying the CTS layer with FF, V_{oc}, J_{sc}, and η are shown in Figure 3. In general, all solar cells' performance increased with an increase in CTS layer thickness. The CdS layer thickness is set to 40 nm while CC is set to 1´10^{15} cm^{-3}.

An increase in CT thickness from 600 nm to 1,500 nm resulted in the rise in efficiency from 16.01% to 19.29%, respectively. This improvement is attributed to the thicker absorber layer's ability to capture more photons, thereby generating more electron-hole pairs (Lin *et al.*, 2014). However, Figure 3 (c) shows that J_{sc} increases insignificantly as thickness increases

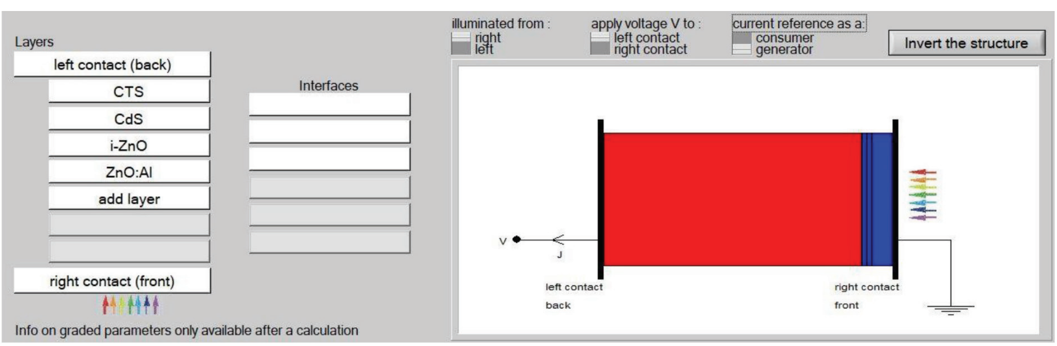

Figure 2: The schematic diagram of the simulated solar cell

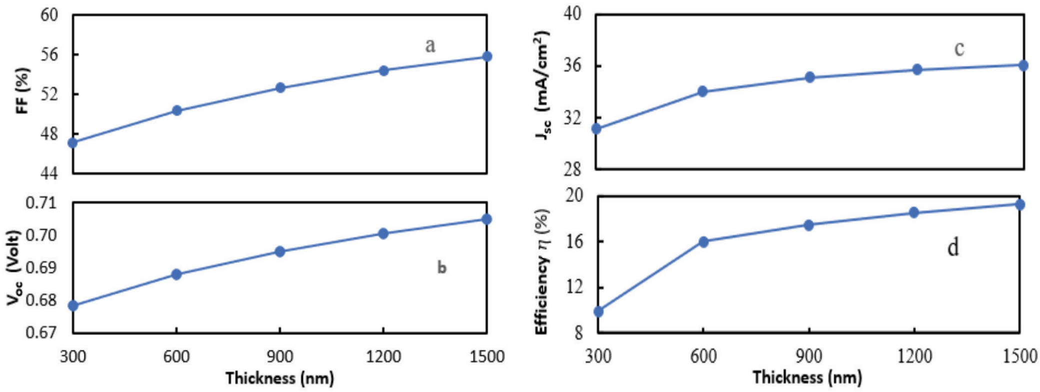

Figure 3: SCAPS-1D analysis of (a) FF, (b) V_{oc}, (c) J_{sc}, and (d) η with varying thicknesses of the CTS layer

beyond 1,200 nm due to photon recombination. In contrast, at thickness below 900 nm, the back contact remains very near to the depletion region, facilitating easier collection of recombined electrons and thereby reducing J_{sc}.

Previous studies have reported that increasing the thickness beyond 1,500 nm lead to only slight gains in efficiency (Shafi *et al*., 2022; Zakaria *et al*., 2023), but a substantial increase in associated costs. Therefore, considering the balance between cost and performance, a maximum thickness of 1,500 nm is considered a justified choice in this study. Although the increase in J_{sc} was proportional to the change in V_{oc}, both are limited by the thickness of CTS. The highest efficiency achieved was 19.29% at 1,500 nm.

CTS Absorber Layer - Effect of Band Gap, E_g

As mentioned earlier, the band gap energy range of CTS solar cells in this study was evaluated from 0.90 eV to 1.20 eV. In this numerical investigation, four different band gap values—0.90 eV, 1.0 eV, 1.10 eV, and 1.20 eV—were tested, with the absorber layer thickness fixed at 1,500 nm.

As the band gap energy increases, the performance of the CTS solar cell improves. As shown in Figures 4 (b) and 4 (c), both FF and V_{oc} rise with increasing band gap while J_{sc} decreases. This trend is expected, as lower bandgap energy enables absorption of a broader range of the solar spectrum, including longer wavelengths, leading to the generation of a higher number of electron-hole pairs. While a lower bandgap energy can increase J_{sc}, it can also lead to a lower open-circuit voltage (V_{oc}) due to the relationship between the band gap and the maximum achievable voltage.

Hence, a trade-off exists between J_{sc} and V_{oc} and the overall power conversion efficiency depends on the balance between these two parameters. As shown in Figure 4 (d), at a band gap of 0.9 eV and 1.2 eV, the calculated efficiency is 9.8% and 14.46%, respectively. Therefore, the optimum value of the CTS layer was achieved for a band gap of 1.2 eV. The performance increase could be attributed to the reduced charge carrier recombination rates in absorber layers with higher band gap energy.

CTS Absorber Layer – Effect of Carrier Concentration, CC

The Carrier Concentration (CC) in the CTS absorber layer were varied from 10^{13} to 10^{18} cm^{-3} as shown in Figure 5. The FF, V_{oc}, and η parameters increased with higher CC, whereas J_{sc} decreased.

The CC significantly affects J_{sc} in solar cells. A higher CC can enhance light absorption and charge carrier generation, leading to an increase in J_{sc}. However, excessively high CC

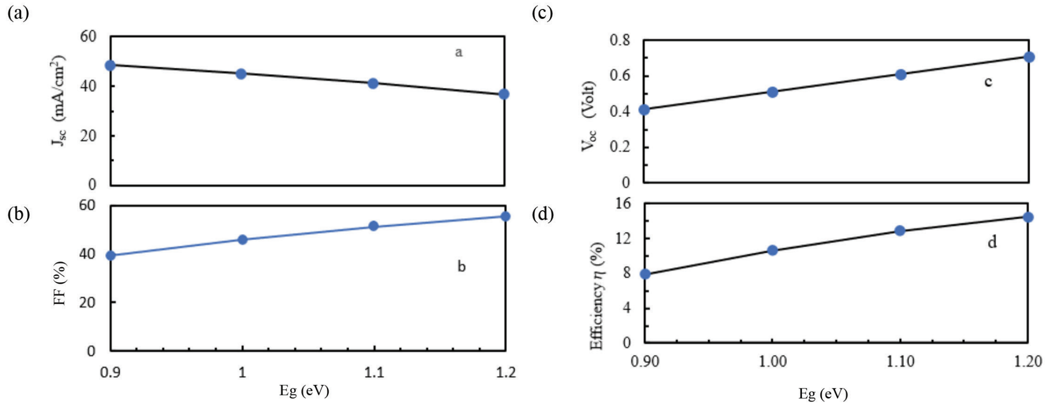

Figure 4: Cell performances in terms of (a) J_{sc}, (b) FF, (c) V_{oc}, and (d) η with varied band gaps of the CTS layer

can also increase recombination, diminishing the benefits. In this study, the highest efficiency was achieved at a CC of 10^{18} cm^{-3}, as shown in Figure 5 (d).

CdS Buffer Layer - Effect of Thickness

This buffer layer lies in between the window and absorber layer, forming the pn junction of the solar cell together with the absorber. The buffer layer facilitates charge transfer across the junction and plays a critical role in improving both performance and stability. In theory, the buffer layer enhances the window-absorber interface, improving crystal quality on both sides and reducing the recombination of holes and electrons. For this analysis, the optimised value of the CTS absorber layer's thickness, E_g and CC was 1,500 nm, 1.2 eV, and 10^{18} cm^{-3} were used.

Figure 6 shows the cell performances with varying thicknesses of the CdS buffer layer from 40 nm to 120 nm. This range was used to investigate the impact of the CdS buffer layer's thickness on solar cell characteristics, which is within the optimum thickness of 60 nm reported by Yamamoto *et al*. (2001). Regardless of the material used, a thin buffer layer typically produces a leakage current while a thick buffer layer could lower the carrier separation rate (Lin *et al*., 2014).

It is observed that increasing the buffer layer thickness causes slight improvements in V_{oc}, J_{sc},

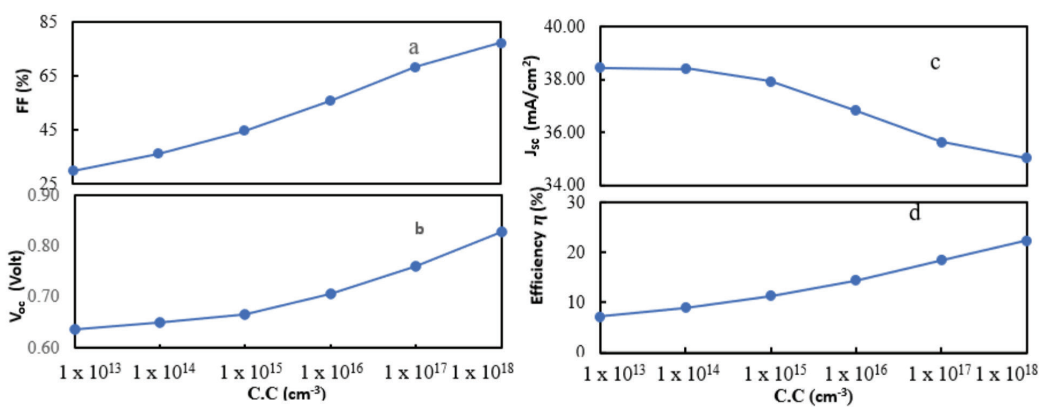

Figure 5: Cell performances in terms of (a) FF, (b) V_{oc}, (c) J_{sc}, and (d) η with varied carrier concentrations of the CTS layer

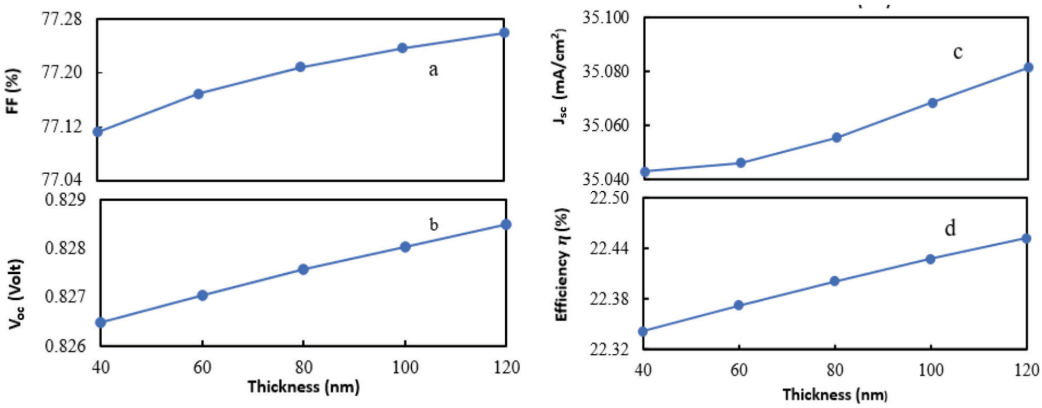

Figure 6: Cell performances in terms of (a) FF, (b) V_{oc}, (c) J_{sc}, and (d) η with varying thicknesses of the CdS layer

FF, and η, as shown in Figure 6. Specifically, efficiency increased slightly from 22.34% to 22.45% as thickness increased from 40 nm to 120 nm. However, the changes in V_{oc}, J_{sc}, FF, or η are not substantial. A thicker buffer layer may absorb higher-energy photons, resulting in photon loss (Chelvanathan *et al*., 2010), as more photons are absorbed by the n-type buffer layer before reaching the p-type absorber layer. This increases the recombination rate, reducing both current and efficiency. Based on the analysis, a buffer thickness of 120 nm is considered optimal, as it does not compromise J_{sc} or V_{oc}.

CdS Buffer Layer – Effect of Carrier Concentration, CC

The Carrier Concentration (CC) of the CdS buffer layer was varied from 10^{12} to 10^{18} cm^{-3}. Figure 7 shows that both V_{oc} and FF begin to decline drastically when the donor concentration exceeds 10^{16} cm^{-3}. As the CC increases, more charge carrier traps are formed, raising the likelihood of contact. Since the charge carrier lifespan is inversely related to trap concentration (Lugue & Hegedus, 2011; Zhang *et al*., 2016), the increased recombination rate reduces the potential difference, leading to a lower V_{oc}.

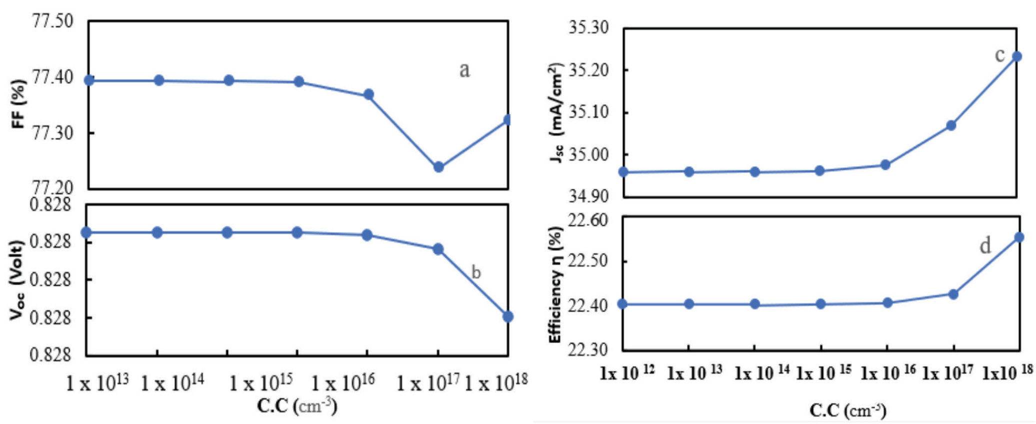

Figure 7: Cell performances in terms of (a) FF, (b) V_{oc}, (c) J_{sc}, and (d) η with varying carrier concentrations of the CdS layer

Consequently, FF, which is proportionally related to V_{oc} also declines. This trend was similarly observed by Zhang *et al.* (2016), where concentrations above 10^{17} cm^{-3} led to a declining pattern that could be explained by the increase in carrier recombination.

In contrast, J_{sc} increases as the carrier concentration increases. This is attributed to an increase in the potential electric field at the heterojunction. As a result, the quantity of photogenerated electron-hole pairs is increased, thereby increasing J_{sc}. The optimal CdS buffer layer CC for an efficient output from a solar cell was found to be 10^{18} cm^{-3}, based on the highest observed η [Figure 7 (d)] of 22.56%. This value corresponds to the most effective doping level for CdS in the simulation.

Comparative Analysis

For comparison, similar results were reported by Amiri *et al*. (2017), who used the same software and achieved a maximum efficiency of 20.36% with a CTS absorber layer thickness of 4,000 nm and a bandgap of 1.25 eV, and a CdS buffer layer thickness of 10 nm. In contrast, this present study improved efficiency to 22.56% by optimising the carrier concentrations in both layers while using a thinner CTS absorber layer of 1,500 nm.

Another study by Hossain *et al*. (2017), using the AMPS-1D software, found optimum CTS absorber layer values of 10^{18} cm^{-3} for carrier concentration and 2,500 nm to 3,000 nm for thickness across different CTS absorber layer phases. For the cubic and tetragonal phases, the optimum absorber layer thickness of 2,500 nm and carrier concentration of 10^{18} cm^{-3} yielded the highest efficiency of 10% and 8%, respectively. For the orthorhombic phase. a thicker absorbing layer of 3,000 nm resulted in an efficiency of 12%.

In terms of experimental outputs, CTS is commonly compared to CZTS solar cells due to their similar compositions. The highest reported experimental efficiency for CTS ranges from 4.6% (Na-doped CTS) to 6.7% (Ge-alloyed CTS) while CZTS has reached 12.6% (Wang *et al*., 2014; Nakashima *et al*., 2015; Umehara *et al*., 2016). A comparable SCAPS-1D simulation by Jiang *et al.* (2019) for Ge-alloyed CTS prediceted an optimum efficiency of 15.65% using a uniform structure. In contrast, this study achieved a simulated efficiency of 22.56%, which is comparatively higher than both the CTS and CZTS existence results, as shown in Table 3. The optimal estimated band gap in this study was 1.2 eV, compared with the experimentally reported CTS band gaps of 1.0 eV to 1.5 eV (Islam *et al*., 2020) and CZTS band gaps of 1.4 eV to 1.6 eV (Islam *et al*., 2021).

The significant discrepancy between the simulated and experimental efficiency values for CTS solar cells is a major concern. The simulation-optimised efficiency of 22.56% greatly exceeds the the experimentally observed values for CTS solar cells, which typically range from 5.1% to 6.7%. While simulations can provide valuable theoretical insights, they often rely on idealised assumptions that may not accurately reflect real-world conditions. This can lead to overly optimistic predictions of device performance. Real-world CTS materials may suffer from defects, impurities, and non-ideal crystal structures, which can significantly degrade performance compared with the perfect

Table 3: CTS simulation comparison

CTS Simulation Result	**CTS's Highest Experimental Result**	**Reference**	**CZTS's Highest Experimental Result**	**Reference**
22.56%	5.1% - 6.7%	(Umehara *et al*., 2016; Chantana *et al*., 2020)	12.6%	(Wang *et al*., 2014)

materials assumed in simulations. Additionally, fabrication variables, including deposition techniques, annealing conditions, and interface engineering can introduce imperfections and limitations that are not accounted for in simulations.

Thin film research while promising, presents several experimental challenges. Achieving precise control over film thickness, composition, and microstructure is often difficult. Ensuring uniform film properties across large areas can be challenging, as variations can significantly impact performance. Minimising defects like grain boundaries, voids, and impurities is crucial for optimising film properties.

Accurately characterising the properties of thin films, especially at the nanoscale, requires highly sensitive techniques. Controlling interfaces between different layers is critical for efficient charge transport and device performance. Ensuring the long-term stability of thin films under various environmental conditions is a major challenge. Scaling up the fabrication process while maintaining consistent quality and cost-effectiveness is a significant hurdle. Compared with other materials, CTS is relatively inexpensive and abundant. It is also non-toxic and environmentally sustainable. However, CTS is still a relatively new material and its long-term stability and scalability need to be fully validated.

Conclusions

The performance of solar cells depends on their internal physical mechanisms. Simulation software allows researchers to predict performance by modelling the physical functioning properties of thin-film solar cells. In this study, a detailed analysis was conducted using SCAPS-1D to model a thin-film solar cell structure comprising Al:ZnO/ZnO/CdS/CTS/Mo/SLG. The performance of the CTS and CdS layers was evaluated by varying their thickness, band gap, and carrier concentration. The optimum values for the CTS absorber layer were identified as a thickness of 1,500 nm, a band gap of 1.2 eV, and a carrier concentration of 10^{18} cm^{-3}. For the CdS buffer layer, the optimum thickness and carrier concentration were both found to be 120 nm and 10^{18} cm^{-3}, respectively.

The optimised structure achieved a J_{sc} of 38.43 mA/cm^2, V_{oc} of 0.83V, FF of 77.32%, and efficiency, η of 22.56%. These results suggest that the proposed CTS/CdS solar cell structure is a promising candidate for photovoltaic applications. The identification of optimum parameter values offers valuable guidance for future fabrication of CTS-based devices, supporting its potential as a green energy solution.

Acknowledgements

This research has been funded by the Universiti Sains Islam Malaysia under USIM Research Grant number PPPI/USIM/FST/USIM/112723. This research is part of a dissertation, which was submitted as partial fulfilment to meet requirements for the degree of Doctor of Philosophy at Universiti Sains Islam Malaysia.

Conflict of Interest Statement

The authors agree that this research was conducted in the absence of any self-benefits, commercial, or financial conflicts and declare the absence of conflicting interests with the funders.

References

Adelifard, M., Mohagheghi, M. M. B., & Eshghi, H. (2012). Preparation and characterisation of Cu2SnS3 ternary semiconductor nanostructures via the spray pyrolysis technique for photovoltaic applications. *Physica Scripta*, *85*(33), 035603. https://doi.org/10.1088/0031-8949/85/03/035603

Aihara, N., Araki, H., Takeuchi, A., Jimbo, K., & Katagiri, H. (2013). Fabrication of Cu2SnS3 thin films by sulfurisation of evaporated Cu-Sn precursors for solar cells. *Physica Status Solidi C*, *10*(7-8), 1086-1092. https://doi.org/10.1002/pssc.201200866

Akcay, N., Gremenok, V. F., Ozen, Y., Buskis, K. P., Zaretskaya, E. P., & Ozcelik, S. (2023). Investigation on photovoltaic performance of Cu2SnS3 thin film solar cells fabricated by RF-sputtered In2S3 buffer layer. *Journal of Alloys and Compounds*, *949*, 169874. https://doi.org/10.1016/j.jallcom.2023.169874

Amiri, I. S., Ahmad, H., Ariannejad, M. M., Ismail, M. F., Thambiratnam, K., Yasin, M., & Nik Abdul Aziz, N. M. A. (2017). Performance analysis of copper tin sulfide, Cu2SnS3 (CTS) with various buffer layers by using SCAPS in solar cells. *Surface Review and Letters*, *24*(6), 1750073. https://doi.org/10.1142/S0218625X17500731

Amlouk, A., Boubaker, K., & Amlouk, M. (2010). A new procedure to prepare semiconducting ternary compounds from binary buffer materials and vacuum-deposited copper for photovoltaic applications. *Vacuum*, *85*(1), 60-64. https://doi.org/10.1016/j.vacuum.2010.04.002

Berg, D. M., Djemour, R., Gütay, L., Siebentritt, S., Dale, P. J., Fontane, X., Izquierdo-Roca, V., & Pérez- Rodriguez, A. (2012). Raman analysis of monoclinic Cu2SnS3 thin films. *Applied Physics Letters*, *100*(19). https://doi.org/10.1063/1.4712623

Bouaziz, M., Amlouk, M., & Belgacem, S. (2009). Structural and optical properties of Cu2SnS3 sprayed thin films. *Thin Solid Films*, *517*(7), 2527-2530. https://doi.org/10.1016/j.tsf.2008.11.039

Chantana, J., Tai, K. Hayashi, H., Nishimura, T., Kawano, Y., & Minemoto, T. (2020). Investigation of carrier recombination of Na-doped Cu2SnS3 solar cell for its improved conversion efficiency of 5.1%. *Solar Energy Materials and Solar Cells*, *206*, 110261. https://doi.org/10.1016/j.solmat.2019.110261

Chelvanathan, P., Hossain, M. I., & Amin, N. (2010). Performance analysis of copper–indium–gallium–diselenide (CIGS) solar cells with various buffer layers by SCAPS. *Current Applied Physics*, *10*(3), S387-S391. https://doi.org/10.1016/j.cap.2010.02.018

Chen, Q., & Ma, D. (2013). Preparation of nanostructured Cu_2SnS_3 photocatalysts by solvothermal method. *International Journal of Photoenergy.* https://doi.org/10.1155/2013/593420

Chen, X., Wang, X., An, C., Liu, J., & Qian, Y. (2003). Preparation and characterisation of ternary Cu–Sn–E (E= S, Se) semiconductor nanocrystallites via a solvothermal element reaction route. *Journal of Crystal Growth*, *256*(3-4), 368-376. https://doi.org/10.1016/S0022-0248(03)01338-1

Fernandes, P. A., Salomé, P. M. P., & Cunha, A. F. (2010). A study of ternary Cu_2SnS_3 and Cu_3SnS_4 thin films prepared by sulfurising stacked metal precursors. *Journal of Physic D: Applied Physics*, *43*, 215403. DOI: 10.1088/0022-3727/43/21/215403

Fiechter, S., Martinez, M., Schmidt, G., Henrion, W., & Tomm, Y. (2003). Phase relations and optical properties of semiconducting ternary sulfides in the system Cu–Sn–S. *Journal of Physics and Chemistry of Solids*, *64*(9-10), 1859-1862. https://doi.org/10.1016/S0022-3697(03)00172-0

Guan, H., Shen, H., Gao, C., & He, X. (2013). Structural and optical properties of Cu_2SnS_3 and Cu_3SnS_4 thin films by successive ionic layer adsorption and reaction. *Journal of Materials Science: Materials in Electronics*, *24*, 1490-1494. https://doi.org/10.1007/s10854-012-0960-x

Han, J., Zhou, Y., Tian, Y., Huang, Z., Wang, X., Zhong, J., Xie. Z., Yang, B., Song, H., & Tang, J. (2013). Hydrazine processed Cu_2SnS_3 thin film and their application for photovoltaic devices. *Frontiers of Optoelectronics*, *7*, 37-45. https://doi.org/10.1007/s12200-014-0389-3

Hossain, E. S., Chelvanathan, P., Shahamadi, S. A., Sopian, K., Bais, B., & Amin, N. (2018). Performance assessment of Cu_2SnS_3 (CTS) based thin film solar cells by AMPS-1D.

Current Applied Physics, *18*(1), 78-89. https://doi.org/10.1016/j.cap.2017.10.009

Islam, M. F., Yatim, N. M., Chelvanathan, P., Ferdaous, M. T., Hashim, M. A., Modak, A. K., & Amin, N. (2020). A critical review of Cu_2SnS_3 (CTS) thin films solar cells. *Malaysian Journal of Science, Health & Technology*, *7*(Special Issues). https://doi.org/10.33102/mjosht.v7i.117

Islam, M. F., Yatim, N. M., & Hashim, M. A. (2021). A review of CZTS thin film solar cell technology. *Journal of Advanced Research in Fluid Mechanics and Thermal Sciences*, *81*(1), 73-87. https://doi.org/10.37934/arfmts.81.1.7387

Jiang, J., Yang, S., Shi, Y., Shan, R., Tian, X., Li, H., Yi, J., & Zhong, J. (2019). Optimisation bandgap gradation structure simulation of $Cu_2Sn_{1-x}Ge_xS_3$ solar cells by SCAPS. *Solar Energy*, *194*, 986-994. https://doi.org/10.1016/j.solener.2019.11.014

Lin, P., Lin, L., Yu, J., Cheng, S., Lu, P., & Zheng, Q. (2014). Numerical simulation of Cu_2ZnSnS_4-based solar cells with In2S3 buffer layers by SCAPS-1D. *Journal of Applied Science and Engineering*, *17*(4), 383-390. https://doi.org/10.6180/jase.2014.17.4.05

Luque, A., & Hegedus, S. (2011). *Handbook of photovoltaic science and engineering*. John Wiley & Sons.

Mathews, N., Tamy Benítez, J., Paraguay-Delgado, F., Pal, M., & Huerta, L. (2013). Formation of Cu2SnS3 thin film by the heat treatment of electrodeposited SnS–Cu layers. *Journal of Materials Science: Materials in Electronics*, *24*, 4060-4067. https://doi.org/10.1007/s10854-013-1361-5

Robles, V., Trigo, J., Guillén, C., & Herrero, J. (2015). Copper tin sulfide (CTS) absorber thin films obtained by co-evaporation: Influence of the ratio Cu/Sn. *Journal of Alloys and Compounds,*, *642*, 40-44. https://doi.org/10.1016/j.jallcom.2015.04.104

Shafi, M. A., Bibi, S., Khan, M. M., Sikandar, H., Javed, F., Ullah, H., Khan, L., & Mari, B. (2022). A numerical simulation for efficiency enhancement of CZTS-based thin film solar cell using SCAPS-1D. *East European Journal of Physics*, *2*, 52-63. https://doi.org/10.26565/2312-4334-2022-2-06

Taher, B., Alias, M., Naji, I., Alawadhi, H., & Al-Douri, A. (2015). Role of substrate temperature and pH value on the topology and morphology characterisations for nano thin Cu_2SnS_3 Films Prepared by CBD Technique. *Australian Journal of Basic and Applied Sciences*, *9*(20), 406-411.

Umehara, M., Tajima, S., Aoki, Y., Takeda, Y., & Motohiro, T. (2016). Cu2Sn1− xGexS3 solar cells fabricated with a graded bandgap structure. *Applied Physics Express*, *9*(7), 072301. https://doi.org/10.7567/APEX.9.072301

Wang, W., Winkler, M. T., Gunawan, O., Gokmen, T., Todorov, T. K., Zhu, Y., & Mitzi, D. B. (2014). Device characteristics of CZTSSe thin-film solar cells with 12.6% efficiency. *Advanced Energy Materials*, *4*(7), 1301465. https://doi.org/10.1002/aenm.201301465

Wu, C., Hu, Z., Wang, C., Sheng, H., Yang, J., & Xie, Y. (2007). Hexagonal Cu_2SnS_3 with metallic character: Another category of conducting sulphides. *Applied Physics Letters*, *91*(14). https://doi.org/10.1063/1.2790491

Yamamoto, Y., Saito, K., Takahashi, K., & Konagai, M. (2001). Preparation of boron-doped ZnO thin films by photo-atomic layer deposition. *Solar Energy Materials and Solar Cells*, *65*(1-4), 125-132. https://doi.org/10.1016/S0927-0248(00)00086-6

Zakaria, S., Mahboub, E. E., & Hichou, A. E. (2023). Physical properties of the low-cost CZTS absorber layer deposited by spin-coating: Effect of the copper concentration associated with SCAPS-1D simulation. *RSC Advances*, *13*(39), 27106-27115. https://doi.org/10.1039/D3RA03996J

Zhang, H., Cheng, S., Yu, J., Zhou, H., & Jia, H. (2016). Prospects of Zn (O, S) as an alternative buffer layer for Cu_2ZnSnS_4 thin-film solar cells from numerical simulation. *Micro & Nano Letters*, *11*(7), 386-390. https://doi.org/10.1049/mnl.2016. 0130